VOL. 23, NO. 2, 2024, 130-135
elektrika.utm.my
ISSN 0128-4428

ELEKTRIKA
Journal of Electrical Engineering

Performance Evaluation of Reconfigurable Intelligent Surfaces-Assisted Millimeter-Wave Network Using Stochastic Geometry-Based Model

Mohammed Mehdi Saleh[1,2], **Nor Aishah Muhammad**[3*], **Norhudah Seman**[1] and **Marwan Hadri Azmi**[1]

[1]Wireless Communication Centre (WCC), Faculty of Electrical Engineering, Universiti Teknologi Malaysia, 81310 UTM Johor Bahru, Johor, Malaysia.
[2]Education College-Qaim, University of Anbar, 55 Ramadi, Al Anbar, Iraq.
[3]Telecommunication Software and Systems (TeSS), Faculty of Electrical Engineering, Universiti Teknologi Malaysia, 81310 UTM Johor Bahru, Johor, Malaysia.

[*]Corresponding author: noraishah@fke.utm.my

Abstract: Millimeter-wave (mm-wave) bands have received significant attention due to their large bandwidth and high frequency. However, mm-wave signals experience high attenuation primarily as a result of their high directivity and vulnerability to blockage, leading to non-line-of-sight (NLOS) conditions and signal outages. Buildings, structures, and natural obstacles can cause signal blockage, which increases connection challenges and creates coverage gaps. A reconfigurable intelligent surface (RIS) is a potential technique that can improve the coverage of mm-wave networks by intelligently reconfiguring the wireless propagation environment. RIS offers novel solutions to blockage issues by passively reflecting and rerouting mm-wave signals in desired directions. This paper presents a simulation-based evaluation of the signal-to-interference ratio coverage probability in RIS-assisted mm-wave networks based on stochastic geometry. We will use random shape theory to represent the blockages within the network. Furthermore, the impact of increasing the density of RIS and the number of reflective elements on network performance will be examined. The results show that RIS can enhance network coverage and decrease the effects of blockages, with considerable increases in coverage probability when compared to networks without RISs.

Keywords: Stochastic Geometry, Reconfigurable Intelligent Surfaces, Millimeter-wave, Signal-to-Interference Ratio

© 2024 Penerbit UTM Press. All rights reserved

Article History: received 21 February 2024; accepted 16 August 2024; published 29 August 2024

1. INTRODUCTION

Fifth-generation (5G) wireless networks have revolutionized communication by providing ultra-fast data rates, minimal latency, and extensive connectivity. 5G networks utilize new technologies and frequency bands, such as millimeter-wave (mm-wave) frequencies, to meet the growing demand for reliable and high-speed wireless communication. As a crucial technology for 5G networks, mm-wave communication offers ample spectrum resources and the potential for exceptionally high data speeds [1]. However, mm-wave networks face significant challenges that limit their coverage range. One of the key challenges facing mm-wave frequencies is the increased susceptibility to blockage due to the short wavelengths [2]. Buildings, trees, and even human bodies can easily attenuate the mm-wave signals, potentially leading to complete signal blockage. Consequently, the coverage of mm-wave networks becomes limited, requiring the deployment of numerous cellular base stations (BSs) to ensure reliable connectivity.

Reconfigurable intelligent surfaces (RIS) have been proposed as a solution to tackle these challenges and enhance the performance of mm-wave networks [3]. RISs, also often referred to as intelligent reflecting surfaces or meta-surfaces, are composed of many passive elements that can be electrically controlled to change the reflection and transmission characteristics of electromagnetic waves [4]. By intelligently manipulating the wave propagation environment, RIS can increase signal strength and coverage range and mitigate the influence of blockage in mm-wave networks [3].

1.1 Related Works

Several studies consider using RISs in the context of stochastic geometry-based mm-wave networks for coverage analysis. In [3], the authors derived the signal-to-interference ratio (SIR) coverage probability in a blockage-free environment, considering interference solely from BSs. The small-scale fading of the RIS-assisted link was modeled using Rayleigh fading, and the product-distances model was assumed for far-field communication. In [5], the authors derived the channel power distribution and subsequently used the derivations of the signal and interference power distributions to evaluate the network coverage probability. However, they did not consider the effect of blockages in their analysis.

In [6], the authors assumed that the direct link between the BS and the user had been blocked and that the user could only communicate via the LOS link through the RIS. The outage probability and ergodic rate were analyzed using a stationary single BS and a single RIS, assuming that the users are distributed in the area according to homogeneous Poisson point processes (PPPs). The work in [7] focused on two scenarios involving small-sized RISs with high deployment density and another involving large-sized RISs with low deployment density. The coverage probability was analyzed as a function of network parameters and blockage densities by using a stationary single BS and a single user, and the RISs were assumed to be distributed in the area according to homogeneous PPPs. The studies in [8], [9] involved using a line Boolean model to represent network blockages. This model assumes that the buildings have zero width and that their centers are distributed with homogeneous PPPs. These works adopted the sum-distance model for the path loss of the RIS-assisted link.

Note that the path loss based on the sum distance or product distance can significantly impact the performance of RIS-assisted communication [10]. The sum-distance model is appropriate for free-space propagation with a large ideal electric conductor but is typically inappropriate for the RIS-assisted link [11]. Furthermore, the received power is unaffected by the size of the RIS, which is considered infinitely large in an asymptotic sense. In contrast, the product distance model assumes that the size of RIS is relatively small compared to the transmission distances, resulting in increased received power as the RIS size increases [12]. In the context of blockage, the line Boolean model assumes that the midpoints of the blockages are modeled as a PPP and that the blockage's length, width, and orientation are uniformly distributed. Due to the above, this model has the drawback of oversimplifying the complexity and variability of real-world environments [8]. This can lead to inaccuracies in predicting the performance of mm-wave wireless networks, especially in urban areas where buildings and other structures vary in size and are not uniformly distributed [13].

1.2 Contributions

In this paper, the performance of a typical user in RIS-assisted mm-wave networks will be evaluated using stochastic geometry tools in the presence of randomly located/shaped blockages. Additionally, we will investigate the effect of increasing the density of RIS and the number of reflective elements on the SIR coverage probability. The paper aims to offer guidelines for the optimal deployment of RISs and the configuration of RIS reflective elements to enhance network performance by conducting simulation-based evaluations.

2. SYSTEM MODEL

This section outlines the system model for evaluating the SIR coverage probability in RIS-assisted mm-wave networks. Simulations will be conducted to examine the impact of different system parameters on network performance, focusing on a typical outdoor user located in the center of the area.

2.1 Network Model

The downlink mm-wave network consists of BSs, RISs, and user devices. The BSs are randomly distributed in a two-dimensional (2D) area, following homogeneous PPPs denoted by Φ_{BS}, with an intensity λ_{BS}. At the same time, the distribution of RISs follows another homogeneous PPPs referred to as Φ_{RIS}, which is independent of Φ_{BS}, with an intensity λ_{RIS}. The users are randomly distributed in the area where each user will be connected to the closest BS and RIS, as shown in Figure 1.

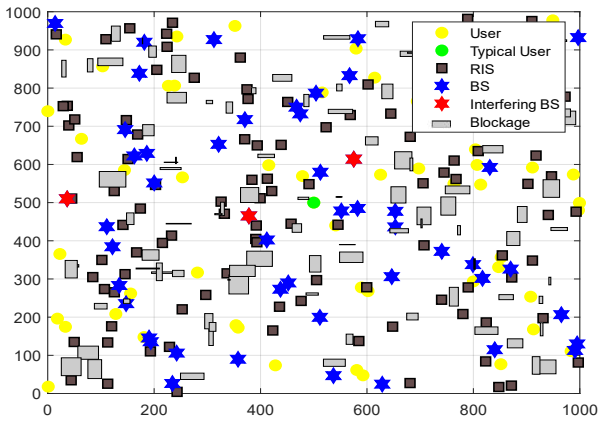

Figure 1. RIS-assisted mm-wave cellular networks.

There are two paths from the BS to the user. The first path is direct from the BS to the user, known as the BS-user path. The second path involves the signal passing via the RIS and then being reflected towards the user, known as the BS-RIS-user path. We will assume perfect beam alignment between the BS and the typical user, as well as between the RIS and the BS and between the RIS and the typical user. Assuming that the buildings completely block the way, we will concentrate on the scenario where the BSs and users are outside. The mm-wave link can exist in either a line of sight (LOS) or a non-line of sight (NLOS) condition [14]. We will assume that the link between the BS and RIS is always LOS, while the link between the BS and the typical user and the link between the RIS and the typical user can be either LOS or NLOS. Based on the blockage model presented in [15], the probabilities of having LOS and NLOS links are denoted as $p_L(\mathrm{r}) = e^{-\beta r}$ and $p_N(r) = 1 - p_L(\mathrm{r})$, respectively. Here, r is the distance between the entities (where $r = r_0$ represents the distance between the BS and the user, and $r = r_2$ represents the distance between the RIS and the user), and β is the blockage factor contingent upon the density and average dimensions of the surrounding buildings.

2.2 Antenna Model

Each BS with n_t isotropic elements can generate two beams directed toward the user and RIS. Each beam has a width of φ_0, which is defined as $\varphi_0 = 2\pi/\sqrt{n_t}$ [16]. Assume that each user has a single omnidirectional antenna and that each RIS has M passive reflective elements.

2.3 Channel and Propagation Model

We will explain the channel model to the typical user while maintaining its generality. The small-scale fading, denoted by g, is assumed to be modeled according to an exponential distribution with a mean of 1 [17]. The mm-wave signal from LOS BS propagates similarly to conditions in free space, while the mm-wave signal from NLOS BS often experiences a higher path loss exponent [14]. We define αL as the path loss exponent for the LOS link and αN as the path loss exponent for the NLOS link, these exponents represent the rate at which the received signal power decreases with distance for the LOS and NLOS links, respectively. The signal received by the typical user from the serving BS can be represented using the model described in [16], considering the distance-dependent path loss for both LOS and NLOS scenarios as follows

$$S_{BS}^{st} = \begin{cases} P_s G_0 r_0^{-\alpha L} & \text{for LOS} \\ P_s G_0 r_0^{-\alpha N} & \text{for NLOS'} \end{cases} \quad (1)$$

Where st indicates whether the link condition is LOS or NLOS, with $st = \{\text{L}, \text{N}\}$, P_s is transmitted power, r_0 represent the distance between the typical user and the serving BS and G_0 represent the small-scale fading gain for the signal sent from the serving BS to the typical user, where $G_0 \sim exp(1)$. This paper focuses on interference signals that come from interfering BSs that have a main beam lobe directed toward the typical user with intensity $\lambda_I = 2\pi/n_t$ [3]. Let S_I be the sum of the interference signals power received by the typical user from all the interferer BSs, which can be expressed as follows

$$S_I^{st} = \begin{cases} \sum_{\substack{BS_i \in \Psi_I \\ i \neq 0}} P_s G_i r_i^{-\alpha L} & \text{for LOS} \\ \sum_{\substack{BS_i \in \Psi_I \\ i \neq 0}} P_s G_i r_i^{-\alpha N} & \text{for NLOS} \end{cases}, \quad (2)$$

where $i = 0$ denote the serving BS, G_i is the small-scale fading gain for the transmitted signal from the interferer BS_i for all i, where $G_i \sim exp(1)$, and r_i is the distance between the typical user and the ith interferer BS. Let S_{RIS} be the signal transmitted from the serving BS to the serving RIS and then to the typical user. This signal can be expressed as follows

$$S_{RIS}^{st} = \begin{cases} P_{RIS} H_1 r_1^{-\alpha L} & \text{for LoS} \\ P_{RIS} H_1 r_1^{-\alpha N} & \text{for NLoS'} \end{cases} \quad (3)$$

where P_{RIS} represent the impinging signal power at the mth passive reflective element where $P_{RIS} = M^2 H_2 r_2^{-\alpha L}$, $H_1$is the small-scale fading gain of the signal transmitted from the serving BS to the serving RIS, $H_1 \sim exp(1)$, H_2 is the small-scale fading gain of the signal transmitted from serving RIS to the typical user, $H_2 \sim exp(1)$, r_1 is the distance between serving BS and the serving RIS, and r_2 is the distance between the serving RIS and the typical user.

2.4 Signal to Interference Ratio (SIR)

The SIR of the received signal through the BS-user link, which is denoted as SIR_{BS}, is given by

$$SIR_{BS} = \frac{S_{BS}^{st}}{S_I^{st}}. \quad (4)$$

In contrast, the SIR of the received signal through the BS-RIS-user link, which is denoted as SIR_{RIS}, is given by

$$SIR_{RIS} = \frac{S_{RIS}^{st}}{S_I^{st}}. \quad (5)$$

Then, the SIR for the typical user, considering the diversity to facilitate the utilization of the receptions through two links: BS-user and BS-RIS-user at the receiver, is given by

$$SIR_t = max(SIR_{BS}, SIR_{RIS}). \quad (6)$$

3. SIR COVERAGE PROBABILITY

The SIR coverage probability can be defined as the probability of the SIR, which can be considered a random variable, being greater than a predetermined threshold γ. Then, the SIR coverage probability is given by

$$CP = P(SIR_t > \gamma) \quad (7)$$

4. MONTE CARLO SIMULATION

In this section, we will outline the main simulation steps shown in Figure 2. We utilize a Monte Carlo simulation and execute these simulations using MATLAB. The locations of BSs and RISs are randomly generated in a 2D area using two independent homogeneous PPPs, assuming the mm-wave network covers a rectangular region with an area of $A = XY$, where X and Y indicate the rectangle's width and length, respectively. Subsequently, users are distributed randomly within the same region, independently of BSs or RISs. Given the assumption that each BS can only serve one user at a time and the total number of users in the network is equal to the number of BSs. The typical user is in the center of the coverage area with coordinates $(X/2, Y/2)$. The typical user will be associated with the closest BS and RIS. We will follow the methodology outlined in Sections 2 and 3 for SIR and SIR coverage probability.

5. PERFORMANCE EVALUATION

In this paper, we evaluate our Monte Carlo simulation of an mm-wave cellular network assisted by RIS using stochastic geometry by comparing the simulation results with the analytical results provided in [3]. Monte Carlo simulations are utilized in this paper within a 1km x 1km square area. The outcomes of these simulations are derived by averaging over 10^4 realizations. During each iteration of the simulation, both BSs and RISs are randomly distributed using homogeneous PPPs with specified intensities. Likewise, UEs are also dispersed randomly within the same area, with the typical user positioned at the center of the region. It should be noted that, unless otherwise specified, we follow the simulation parameters listed in Table 1.

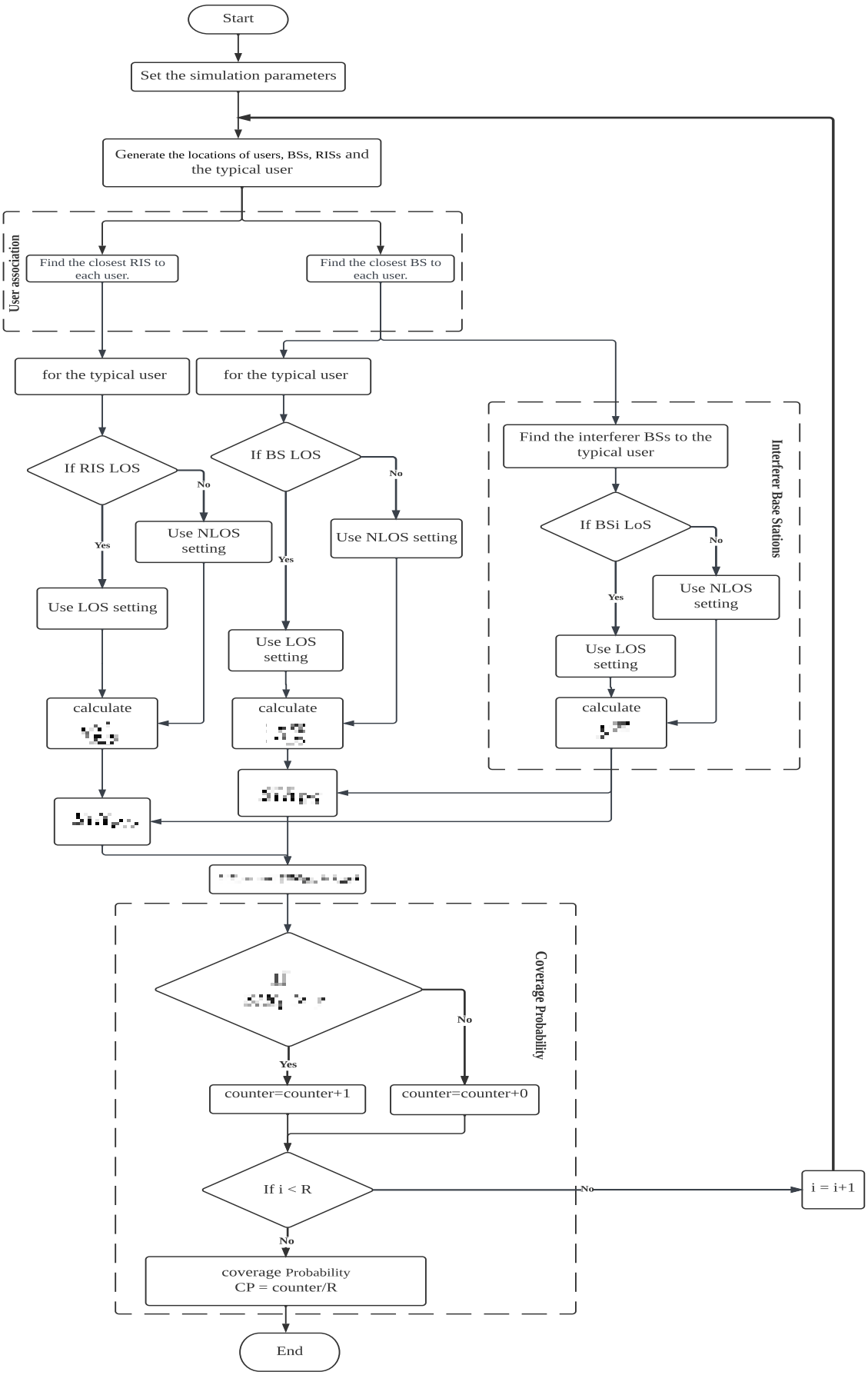

Figure 2: Simulation flowchart.

Table 1: System Numerical Parameters [3], [15]

System parameters	Notation	Value
LOS Path loss exponent	αL	2
NLOS Path loss exponent	αN	4
BS radiated power	P_s	2 w
Blockage factor	β	0.0071
BS antenna array	n_t	16
UE antenna array	n_r	1
RIS reflective elements	M	100, 200
Small-scale channel gain	G_i, H_1,H_2	$\sim exp$ (1)

5.1 Evaluation of Monte Carlo Simulation and Its Effectiveness

Figure 3 shows the results of our Monte Carlo simulation and the results obtained from the analytical framework outlined in [3], particularly utilizing approximation II (51) for scenarios with RIS and (6) for scenarios without RIS. The findings demonstrate perfect alignment between the analytical and simulation results, confirming the accuracy of our simulation methodology. The simulation was conducted without considering blockage effects and utilized a path loss exponent α = 4. The simulation parameters listed in TABLE 1 were followed for the remaining specifications.

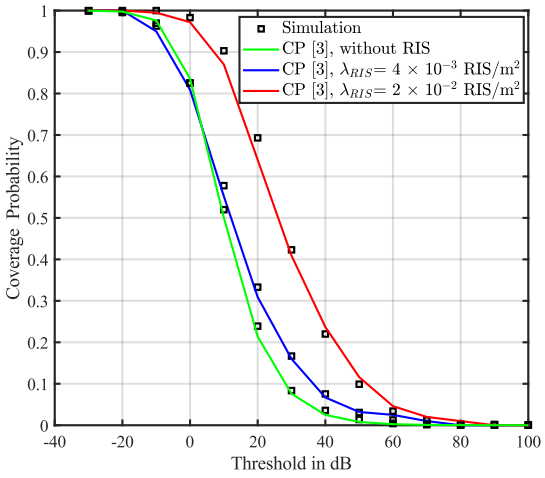

Figure 3. Evaluation of SIR coverage probability $\lambda_{BS} = 2.5 \times 10^{-5}\ BS/m^2$ and $M = 100$ *and* $\alpha = 4$.

5.2 Impact of Blockage on SIR Coverage Probability

The path loss exponent (α) measures how rapidly signal strength drops over distance. In [3], a high fixed value of α is utilized to simulate obstruction effects in urban environments. However, considering the shape and location of physical obstacles in the study results in a more realistic picture of the environment's impact on signal propagation. In [3], the authors utilized α = 4 as a fixed value. In this paper, we use a random rectangular blockage model with β = 0.0071 and two different α values for LOS and NLOS conditions. Figure 4 shows the results of our Monte Carlo simulation for an RIS-assisted mm-wave cellular network using stochastic geometry in blockage scenarios. The results show that the SIR coverage probability (CP) increases significantly with an increase in RIS density. This is because as the density of RIS increases, the likelihood of having a close LOS RIS to a user increases, resulting in a reduction in the value and variance of the distance between a typical user and RIS. This leads to mitigating the effects of blockages.

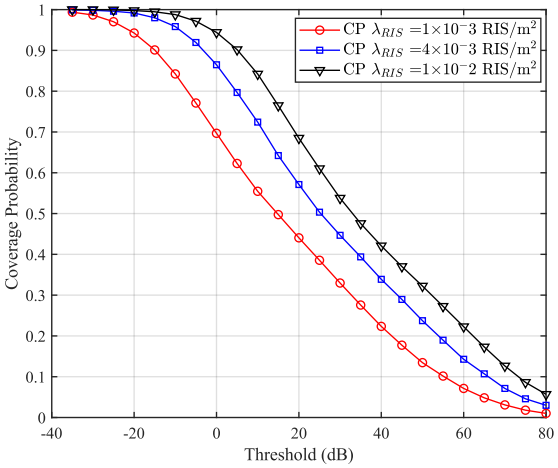

Figure 4. SIR coverage probability using a rectangular blockage model with $\beta = 0.0071$, $\lambda_{BS} = 2.5 \times 10^{-5}\ BS/m^2$ and $M = 100$.

In Figure 5, we illustrate the effect of both increasing the number of reflective elements in the RIS and increasing the density of the RIS on the SIR coverage probability. The results show that CP increases as the number of reflective elements increases. This is because equipping the RIS with a large array of reflective elements enables the generation of more narrowly focused beams with higher gain directed toward the typical user. This improves signal propagation and consequently increases the strength of the received signal, resulting in CP approaching one.

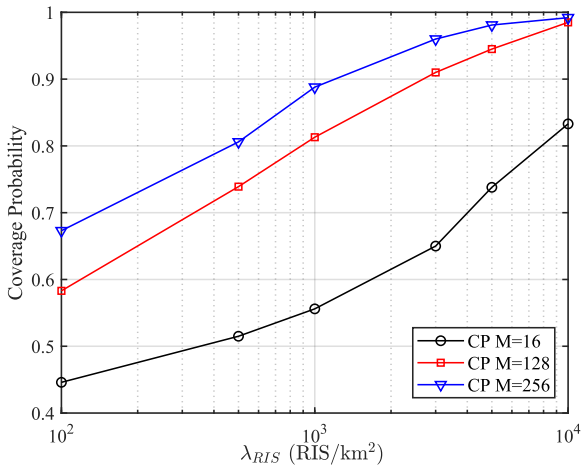

Figure 5. SIR coverage probability using a rectangular blockage model with $\gamma = 0\ dB$, $\beta = 0.0071$ and $\lambda_{BS} = 2.5 \times 10^{-5}\ BS/m^2$.

6. CONCLUSION

In this paper, based on stochastic geometry, we evaluate the SIR coverage probability in RIS-assisted mm-wave networks, taking into consideration the effects of blockage. We conduct simulation-based evaluations following the system model proposed in [3] and utilize the rectangular blockage model proposed in [15] to examine the impact of blockage on SIR coverage. Our findings demonstrate the importance of using RIS to address blockage challenges. We also highlight the positive influence of increasing RIS density and/or the number of reflective elements on enhancing CP and expanding the coverage area. Our future work will expand based on this foundation to investigate how RISs could be used to overcome direct obstacles by providing indirect links between BSs and UEs.

ACKNOWLEDGMENT

This work was supported in part by the Ministry of Higher Education (MOHE) Malaysia through the Fundamental Research Grant Scheme (FRGS), Grant No.: FRGS/1/2023/TK07/UTM/02/12 and HICoE Grant (R.J130000.7809.4J613).

REFERENCES

[1] N. K. Mallat, M. Ishtiaq, A. Ur Rehman, and A. Iqbal, "Millimeter-Wave in the Face of 5G Communication Potential Applications," IETE Journal of Research, vol. 68, no. 4. 2022. doi: 10.1080/03772063.2020.1714489.

[2] A. N. Uwaechia and N. M. Mahyuddin, "A comprehensive survey on millimeter wave communications for fifth-generation wireless networks: Feasibility and challenges," IEEE Access, vol. 8, 2020, doi: 10.1109/ACCESS.2020.2984204.

[3] M. Nemati, J. Park, and J. Choi, "RIS-Assisted Coverage Enhancement in Millimeter-Wave Cellular Networks," IEEE Access, vol. 8, 2020, doi: 10.1109/ACCESS.2020.3031392.

[4] C. Huang, A. Zappone, G. C. Alexandropoulos, M. Debbah, and C. Yuen, "Reconfigurable intelligent surfaces for energy efficiency in wireless communication," in IEEE Transactions on Wireless Communications, 2019. doi: 10.1109/TWC.2019.2922609.

[5] J. Lyu and R. Zhang, "Hybrid active/passive wireless network aided by intelligent reflecting surface: System modeling and performance analysis," IEEE Transactions on Wireless Communications, vol. 20, no. 11, 2021, doi: 10.1109/TWC.2021.3081447.

[6] T. Hou, Y. Liu, Z. Song, X. Sun, Y. Chen, and L. Hanzo, "MIMO Assisted Networks Relying on Intelligent Reflective Surfaces: A Stochastic Geometry Based Analysis," IEEE Transactions on Vehicular Technology, vol. 71, no. 1, 2022, doi: 10.1109/TVT.2021.3129308.

[7] Z. Li, H. Hu, J. Zhang, and J. Zhang, "RIS-Assisted mmWave Networks with Random Blockages: Fewer Large RISs or More Small RISs?," IEEE Transactions on Wireless Communications, vol. 22, no. 2, 2023, doi: 10.1109/TWC.2022.3200157.

[8] M. A. Kishk and M. S. Alouini, "Exploiting Randomly Located Blockages for Large-Scale Deployment of Intelligent Surfaces," IEEE Journal on Selected Areas in Communications, vol. 39, no. 4, 2021, doi: 10.1109/JSAC.2020.3018808.

[9] S. Bagherinejad, M. Bayanifar, M. Sattari Maleki, and B. Maham, "Coverage probability of RIS-assisted mmWave cellular networks under blockages: A stochastic geometric approach," Physical Communication, vol. 53, 2022, doi: 10.1016/j.phycom.2022.101740.

[10] Y. Cheng, W. Peng, C. Huang, G. C. Alexandropoulos, C. Yuen, and M. Debbah, "RIS-Aided Wireless Communications: Extra Degrees of Freedom via Rotation and Location Optimization," IEEE Transactions on Wireless Communications, vol. 21, no. 8, 2022, doi: 10.1109/TWC.2022.3151702.

[11] Q. Wu, S. Zhang, B. Zheng, C. You, and R. Zhang, "Intelligent Reflecting Surface-Aided Wireless Communications: A Tutorial," IEEE Transactions on Communications, vol. 69, no. 5, 2021, doi: 10.1109/TCOMM.2021.3051897.

[12] Y. Liu et al., "Reconfigurable Intelligent Surfaces: Principles and Opportunities," IEEE Communications Surveys and Tutorials, vol. 23, no. 3. 2021. doi: 10.1109/COMST.2021.3077737.

[13] A. Y. Etcibasi and E. Aktas, "Coverage Analysis of IRS-Aided Millimeter-Wave Networks: A Practical Approach," IEEE Transactions on Wireless Communications, 2023, doi: 10.1109/TWC.2023.3310664.

[14] N. A. Muhammad, N. Seman, N. I. A. Apandi, and Y. Li, "Energy Harvesting in Sub-6 GHz and Millimeter Wave Hybrid Networks," IEEE Transactions on Vehicular Technology, vol. 70, no. 5, 2021, doi: 10.1109/TVT.2021.3068956.

[15] T. Bai and R. W. Heath, "Coverage and Rate Analysis for Millimeter Wave Cellular Networks," Feb. 2014, [Online]. Available: http://arxiv.org/abs/1402.6430

[16] K. Venugopal, M. C. Valenti, and R. W. Heath, "Interference in finite-sized highly dense millimeter wave networks," in 2015 Information Theory and Applications Workshop, ITA 2015 - Conference Proceedings, 2015. doi: 10.1109/ITA.2015.7308984.

[17] M. Rebato, J. Park, P. Popovski, E. De Carvalho, and M. Zorzi, "Stochastic geometric coverage analysis in mmwave cellular networks with realistic channel and antenna radiation models," IEEE Transactions on Communications, vol. 67, no. 5, 2019, doi: 10.1109/TCOMM.2019.2895850.